Preprints of the 2012 20th Mediterranean Conference on Control & Automation (MED), Barcelona, Spain, July 3-6, 2012

An Actuated Platform FEA Model used for Precision Pointing Control

Gerardo Zarate, Eric Diaz, Jessica Alvarenga, Khosrow Rad, *Members IEEE* and Helen Boussalis, *Senior Member, IEEE*

***Abstract*— A large, segmented space telescope requires high precision and accuracy in its mirror shape to obtain clear images. The Structures, Propulsion, and Control Engineering (SPACE) telescope testbed at the NASA sponsored University Research Center must maintain a pointing control accuracy of 2 arc seconds. A Peripheral Pointing Architecture (PPA) has been designed to demonstrate the testbed pointing accuracy. A finite element model of the PPA is developed. Normal mode analysis is performed to establish the PPA's natural frequencies, mode shapes, mass and stiffness matrices. Utilizing H-infinity controllers developed for figure maintenance, the pointing control of the testbed structure is achieved.**

I. Introduction

Due to an ever increasing need to "see" further into space, a new generation of space telescopes is needed. Younger objects, receding from us at an ever-faster rate, are red-shifted into the near infrared where Hubble loses sensitivity, [1].

To meet this requirement the National Aeronautics and Space Administration (NASA) will replace the Hubble Space Telescope with the James Webb Space Telescope (JWST), previously known as the Next Generation Space Telescope (NGST). This telescope consists of a very large light-gathering primary mirror capable of detecting faint signals from the first billion years, the period when galaxies have been formed. The JWST will be capable of detecting radiation whose wavelength lies in the range of 0.6 to 20 mm. Furthermore, the JWST will be able to see objects 400 times fainter than those currently studied with large ground-based infrared telescopes such as the Keck Observatory.

Manuscript received May 14, 2012. This work was supported in part by NASA under Grant URC NNX08BA44A.

G. Zarate is with the NASA SPACE Center at California State University, Los Angeles, LA, CA 90032 USA, (phone: 323-343-5445; e-mail: gzarate@calstatela.edu).

E. Diaz is with the NASA SPACE Center at California State University, Los Angeles, LA, CA, 90032 USA, (e-mail: ericdiaz@usc.edu).

J. Alvarenga is with the NASA SPACE Center at California State University, Los Angeles, LA, CA, 90032 USA, (e-mail: jalvare5@calstatela.edu).

K. Rad is with the NASA SPACE Center and the Electrical Engineering Department at California State University, Los Angeles, LA, CA 90032 USA, (e-mail: krad@calstatela.edu).

H. Boussalis is with the NASA SPACE Center and the Electrical Engineering Department at California State University, Los Angeles, LA, CA 90032 USA, (e-mail: hboussa@calstatela.edu).

Due to the size and weight limitations associated with current launch vehicles, the Next Generation Space Telescopes will employ segmented reflectors. Although multiple-mirror designs have many advantages, a number of major difficulties are associated with this technique. Due to atmospheric disturbances, the mirrors can be easily misaligned and figure maintenance, as well as, precision pointing of the telescope cannot be achieved. Therefore, to accomplish figure maintenance and precision pointing of the large segmented structure, design of sophisticated controllers is necessary

To study the control of such large segmented optical systems, in 1994, NASA established the SPACE Laboratory at California State University, Los Angeles (CSULA). One of the major goals of this Laboratory is to design and fabricate a testbed that resembles the complex dynamic behavior of a segmented space telescope, [2], [3], [4]. The SPACE center team of students and faculty work on the development of control algorithms which will accomplish the figure maintenance and precision pointing of the control oriented SPACE testbed, [5]. Due to the symmetry of the structure and the nature of the interconnections among its subsystems, decentralized control techniques are utilized.

The SPACE testbed utilizes an actuated laser platform to demonstrate accomplishment of the precision pointing and figure maintenance of the complex structure, [6]. Previous work has shown the achievement of 1 micron RMS figure maintenance of the segmented reflector. To accomplish this requirement, a decentralized H-infinity controller has been developed, [9], and [10]. To achieve the pointing of the SPACE testbed with accuracy of 2 arc seconds, the team is investigating the use of the already established controllers [9], [10]. To utilize the existing control law, first, the actuated laser platform is modeled using finite element techniques.

II. Background

A. SPACE Testbed

The SPACE testbed shown in Fig. 1 emulates a Cassegrain telescope of 2.4-meter focal length with performance comparable to an actual space-borne system. The system's top-level requirements include figure maintenance of the primary mirror to within 1 micron RMS distortion with respect to a nominal shape of the primary mirror, and precision pointing with accuracy of 2 arc seconds, [4], [6], [7].

978-1-4673-2529-5/12/$31.00 ©2012 IEEE

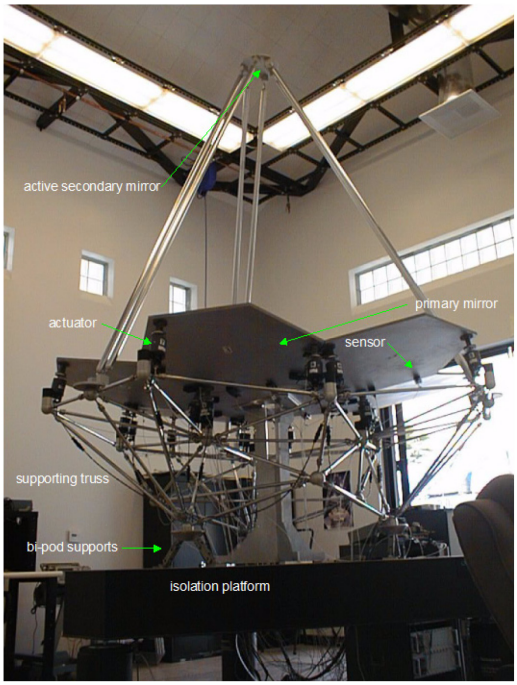

Fig. 1. SPACE Testbed

The SPACE testbed consists of a primary mirror, a secondary mirror and a lightweight flexible truss structure. The primary mirror (mounted on the support truss) consists of seven hexagonal panels, each 101 cm in diameter. The six peripheral panels are actively controlled in the three degrees-of-freedom by 18 linear electromagnetic actuators (3 actuators per active panel), and the seventh panel is used as a reference. In addition, a set of 18 edge sensors are used to provide measurements of relative displacement and angle of the panels (3 sensors per active panel). The Testbed's active secondary mirror is a six-sided pyramidal mirror used to reflect the light from the primary mirror to the central plane and is attached to the primary by a tripod. The entire Testbed is supported by a triangular isolation platform made of aluminum honeycomb core with stainless steel top and bottom skin, [8].

B. *SPACE Testbed Modeling*

The SPACE testbed is composed of six hexagonal segments. Each of these segments is modeled as an equilateral triangle with corners at the panel support points. The panels are attached to the Testbed truss via the support assembles shown in Fig. 2.

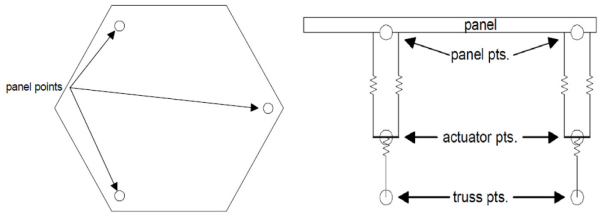

Fig. 2. Panel and Panel Support

Fig. 3 shows the results of modal analysis performed on the finite element model of the Testbed. From this, the global modes were obtained.

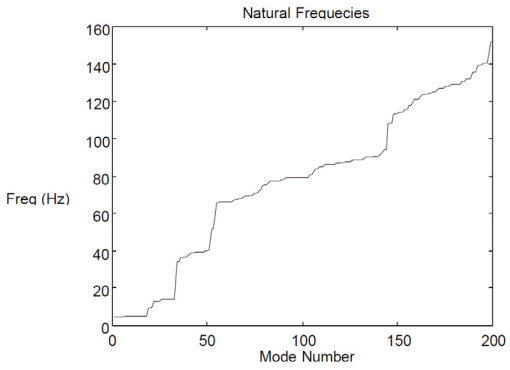

Fig. 3. SPACE Testbed Frequency Histogram

C. *Figure Maintenance*

Unlike a monolithic primary mirror, a segmented reflector, such as the JWST or the SPACE testbed, requires an active control system to maintain the desired optical performance. Active control of the Testbed reflector panels was achieved using an H-infinity controller, Fig. 4, designed to suppress vibrations and provide figure maintenance and shape control of the primary mirror. Fig. 5 shows the closed loop response results, [9], using this control scheme under decentralized control.

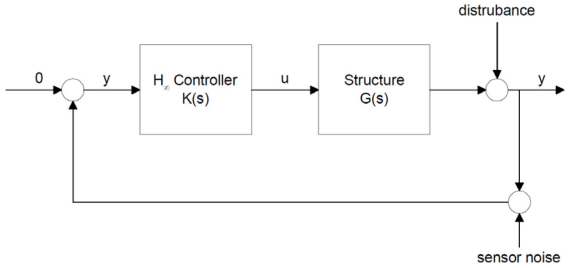

Fig. 4. H-infinity Control Loop

It is evident that figure maintenance is achieved using the decentralized control scheme described in [4], [5], [10].

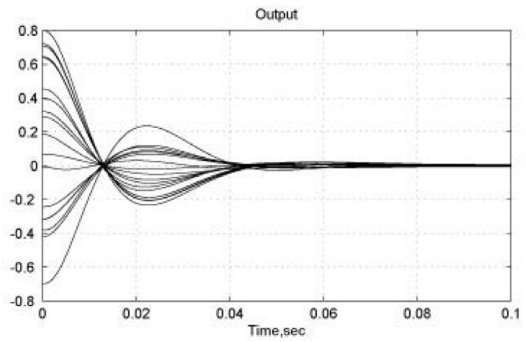

Fig. 5. Closed loop response of the six Testbed panels to the Decentralized H-infinity controller, [9]

D. *Peripheral Pointing Architecture*

The SPACE telescope testbed is required to perform precision pointing while maintaining the parabolic shape of the primary mirror. In order to achieve precision pointing of the Testbed with accuracy of 2 arc seconds, a Peripheral Pointing Architecture (PPA) has been designed Fig. 6. The PPA structure is shown in Fig. 7.

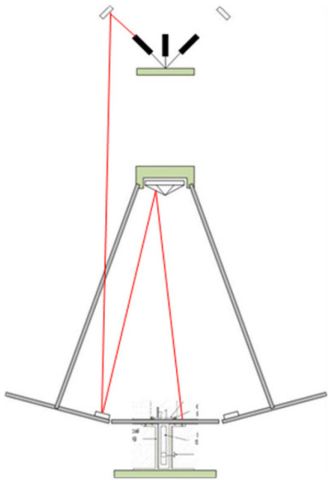

Fig. 6. SPACE Testbed PPA Laser Path

The PPA uses an assembly of six lasers as shown in Fig. 8 to simulate the object of study. Each laser corresponds to its own separate panel and optical detector. The laser assembly sits on a motorized tip/tilt platform and the laser source coincides with the rotation, or gimbal, point of the platform.

Since the laser source lies on the rotation point of the platform, there is no translation or displacement of the source. When the motorized platform is tipped or tilted, the source is stationary, while only the laser beams direction are affected.

Using the distance from the platform's rotation point to each actuator, (a_x and a_y for the actuator on each respective axis), and the actuator displacement, it is calculated that the platform moves an angle θ from its zero position on the y-axis. The platform's normal vector also moves the same angle θ from the positive z-axis.

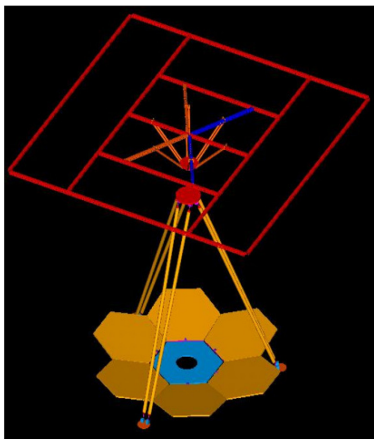

Fig. 7. PPA Structure

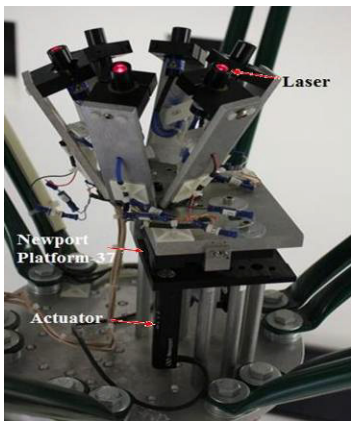

Fig. 8. Laser Assembly

III. Modal Analysis

In mathematical terms, the PPA is described by a set of `equations of motion of the form:

$$M\ddot{\delta} + C\dot{\delta} + K\delta = F \quad (1)$$

where δ represents the degrees of freedom (DOF) and M, C, and K represent the global mass, internal damping, and stiffness matrices respectively, and F represents the input force (or moments) to the system. For the purpose of modeling a very rigid structure like the PPA, the internal damping is excluded (assumed to be very near 0), resulting in a first approximation of the system dynamics, (2).

$$M\ddot{\delta} + K\delta = F \quad (2)$$

With (2) in hand, the model's eigenvalues/frequencies and mode shapes (eigenvectors) can be extracted by solving the eigenvalue problem as stated in (3), obtained by setting the input force F to zero.

$$\ddot{\delta} = -M^{-1}K\delta \quad (3)$$

The eigenvectors of (3) represent the mode shapes of the system which can be compiled together to form a modal matrix, Φ, used to transform (2) into generalized coordinates, q, according to the substitution made in (4). The resulting equation of motion in terms of q is given in (5). To simplify analysis, the mass matrix M can be normalized with respect to the modal matrix (equation 6). Therefore, premultiplying (5) by the transpose of Φ, results in a simplified equation of motion in terms of q in (7).

$$\delta = Mq \quad (4)$$

$$M\Phi\ddot{q} + K\Phi q = F \quad (5)$$

$$\Phi^T M\Phi = I \quad (6)$$

$$\ddot{q} + \Lambda q = \Phi^T F \quad (7)$$

$$\Lambda = \Phi^T K\Phi \quad (8)$$

where Λ, seen in (8), is the system spectral matrix consisting of the eigenvalues of the system.

The simplified representation in (7) allows for the derivation of a mathematical model that can be used to simulate the dynamics of the PPA in software and the straight-forward derivation of a state-space model for the development of a controller. In order to identify all the DOF of interest of the physical model, first a mechanical model is developed in software, which is then meshed and used for finite element analysis (FEA) in solving (3) for the system eigenvalues and mode shapes.

IV. Finite Element Model Development

Development of the PPA FEA Model starts with defining the PPA structure geometry in SolidWorks and saving the model as a parasolid file. The SolidWorks parasolid file is then imported to FEMAP where the material and properties are defined. Mesh analysis is performed on the model and an FEA model is constructed. This FEA model is then imported to NX Nastran for dynamic analysis. Normal mode analysis is performed on the meshed model and NX Nastran outputs degrees of freedom, eigenvalues, natural frequencies and mode shapes of the PPA structure in the form of text files.

A. SolidWorks Model

A geometric model of the PPA is developed using SolidWorks. The PPA structure is composed of six lasers, six laser holders, a hexagonal plate, the top platform, the Newport 37 platform, two Newport linear actuators, and nine supporting rods. These components are assembled together as shown in Fig. 9. The placements of the lasers are determined through a raytracing algorithm, described in [7]. Placing the lasers at this angle allows for all six lasers to originate from the same point at the platform. The units of measurement used for the model are in millimeters.

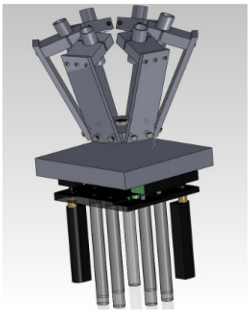

Fig. 9. SolidWorks Model

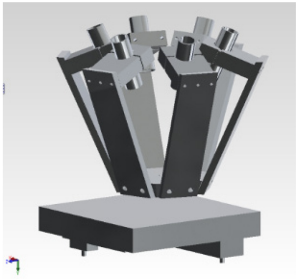

Fig. 10. Updated Solidworks Model

The PPA is composed of two main parts which consist of a controllable and a fixed part. The controllable part is the top half section of the structure where the actuators push upwards in a linear fashion and where the Newport 37 platform has its gimbal point. The fixed part is the bottom half of the structure where the actuators, supporting rods and bottom portion of the Newport 37 platform are located. For simplicity and ease of computation the fixed part of the PPA structure was removed resulting in Fig. 10. To develop the PPA model, first the model for each component is developed. The designed geometry is saved as a parasolid file and imported into Finite Element Modeling and Post Processing (FEMAP).

B. FEMAP Model

The parasolid model developed utilizing SolidWorks is imported into the FEMAP software package to define the elements and properties of the PPA structure. Following, a mesh analysis is performed. The properties are specified to be 6061 Aluminum for the entire structure and are constructed with solid elements for simplicity of design and more accurate results. Mesh analysis is performed on the model resulting with 250000 nodes and 150000 elements. The element growth ratio and mesh density have to be increased using FEMAP's meshing toolbox in order to minimize the number of nodes and elements in the model but a problem arises which affects the accuracy of the results by changing these parameters. Therefore careful selection is placed on which areas of the model would be affected by the increase in element growth ratio and/or mesh density. The element growth ratio is increased throughout the model and the mesh density is increased mostly on the platform and by a small amount on the laser holders. The reason being that the platform has more mass and is more rigid than the laser holders. The minimum number of nodes and elements achieved with keeping reasonably accurate results is 146000 nodes and 91000 elements using solid elements shown in Fig. 11.

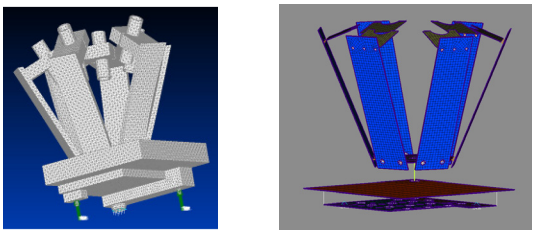

(a) (b)

Fig. 11. FEA Model: Solid Elements (left) Plate Elements (right)

In order to reduce the number of nodes and elements and to minimize computation time another mesh analysis approach is used. In using plate and beam elements, as opposed to solid elements, the number of nodes and elements of the model can be reduced significantly. Therefore, the solid element model is converted to a plate element model resulting in 8819 nodes and 7998 elements. The model is

reduced even further by increasing the element growth ratio and mesh density on the platform and certain areas of the laser holders using the meshing toolbox. Using plate elements and increasing the growth ratio and mesh density the model is reduced to 5795 nodes and 4993 elements.

Constraints are to be applied to finalize the FEA model of the PPA structure. The lasers on the PPA are positioned to have the laser source originate at the rotation point of the platform. The platform is assembled with two linear actuators that provide two axes of tilt. The gimbal point is composed of a hardened and polished steel ball which pivots giving the gimbal point three axis rotational degrees of freedom. Therefore the PPA model is constrained at three points. Two points for the linear actuators are constrained in the x-axis and y-axis for translation and in the x, y, and z axes for rotation. The gimbal point has a pinned constraint meaning that it is cannot translate. This completes the FEA modeling for the PPA structure shown in Fig. 11.

V. Results

By performing modal analysis, the mode shapes and their respective frequencies are obtained showing that the PPA is a rigid structure. NX Nastran outputs a .f06 text file containing the natural frequencies, mode shapes, degrees of freedom, eigenvalues, and other information of the structure. The text file is parsed and only the eigenvalues, eigenvectors, frequencies, and degrees of freedom are extracted.

An initial analysis shows the frequency range for the first 100 modes ranged from 56.7 Hz to 13.017 kHz as shown in Fig. 12. A second analysis yielded similar results, but were truncated to the first 20 modes (approximately 1 kHz), to reduce the size of the eventual state-space model, since it was determined that higher frequencies would not be within the operational range.

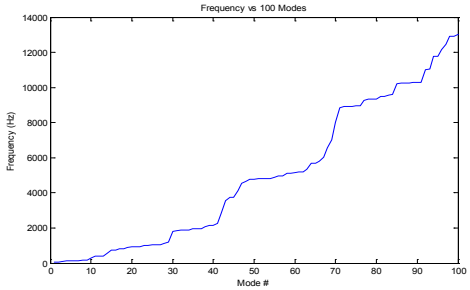

Fig. 12. Frequency of first 100 modes of platform structure

The first group of mode shapes corresponds to deformations of the laser holders followed by the deformation of the platform. The deformations of mode 4 at 126.2326 Hz and mode 10 at 261.7744 Hz are shown in Fig. 13. This figure shows the deformations of the laser holders in the first group of frequencies followed by the more rigid platform at higher frequencies.

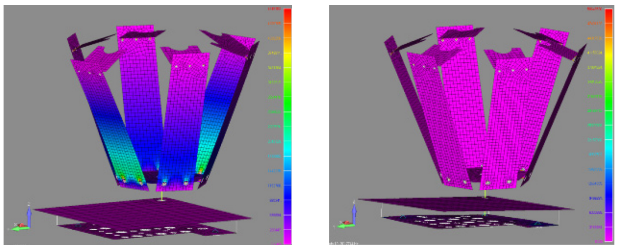

(a) (b)

Fig. 13. Mode 4, 126.2326 Hz (left). Mode 10, 261.7744 Hz (right).

VI. Control Design

Consider the linear time-invariant system given by the following state equations,

$$\dot{x} = Ax + \sum_{i=1}^{v} B_i u_i$$
$$y_i = C_i x, \qquad i = 1, \cdots, N \tag{9}$$

where $x \in \Re^n$, $u_i \in \Re^{m_i}$ and $y_i \in \Re^{p_i}$ represent the state, input and output respectively of the *i*th local control station. A, B_i and C_i are real, constant matrices. The results of the modal analysis are used to determine the matrices A, B_i and C_i that will describe the dynamics of the PPA structure.

For decentralized control, it is necessary to determine n local feedback control laws that will dynamically compensate for (9) in order to stabilize the control loop, generating the following feedback controllers:

$$\dot{z} = F_i z_i + G_i y_i$$
$$u_i = H_i z_i + K_i y_i + v_i, \quad i = 1, \cdots, N \tag{10}$$

Where $z_i \in \Re^{n_i}$ and $v_i \in \Re^{m_i}$ are the *i*th subcontroller and local external input and F_i, G_i, H_i, and K_i are real, constant matrices. The standard two-block mixed-sensitivity H-infinity technique, [9], will be applied to accomplish a pointing accuracy of 2 arc seconds.

VII. Conclusion

An FEA model of an actuated laser platform used for pointing control of a segmented telescope testbed is developed. Modal analysis is performed on the FEA model which calculates the natural frequencies, mode shapes, degrees of freedom, and eigenvalues of the structure. Further research is to be undertaken to define which nodes are desirable and which nodes are unnecessary in order to be able to perform Guyan Reduction to reduce the size of the model for practical implementation.

Acknowledgment

Special thanks go to the SPACE Center faculty and students for their contributions to this work.

REFERENCES

[1] H. S. Stockman, "The Next Generation Space Telescope Visiting a Time When Galaxies Were Young", June 1997.

[2] H. Boussalis, Z. Wei, and M. Mirmirani, "Dynamic Performance Modeling and Decentralization of A Segmented Reflector Telescope," IASTED Conference on Modeling and Simulation, Mexico, 1995.

[3] H. Boussalis, "Decentralization of Large Spaceborne Telescopes", Proc. 1994 SPIE Symposium on Astronomical Telescopes, Hawaii, 1994.

[4] H. Boussalis, M. Mirmirani, A. Chassiakos, K. Rad, "The Use of Decentralized Control in Design of a Large Segmented Space Reflector", Control and Structures Research Laboratory, California State University, Los Angeles, Final Report, 1996.

[5] H. Boussalis, "The Use of Decentralized Control in Design of A Large Segmented Space Reflector", Structure Pointing and Control Laboratory, California State University, Los Angeles, Final Technical Report, 2002.

[6] H. Boussalis, K. Rad, A. Khosafian, Y. Komandyan, "Pointing Control Testbed for Segmented Reflectors", June 2005.

[7] A. Desai, J. Alvarenga, H. Tarsaria, K. Rad, H. Boussalis, "Ray Tracing Visualization Using LabVIEW for Precision Pointing Architecture of a Segmented Reflector Testbed," MED 2011, Corfu, Greece, June 2011.

[8] M. J. Morales, "Design and modeling of the SPACE Tesbted," M.S. Thesis, Department of Electrical Engineering, California State University, Los Angeles, Los Angeles, CA, USA, 2001.

[9] M.J. Morales, M. Mirmirani, H. Boussalis, "Design, Simulation & Control of a Segmented Reflector Test-bed," MED 1999, Haifa, Israel, June 28-30, 1999.

[10] K. Lim, "Modelling and Overlapping Decentralized Control of a Large Segmented Telescope Test-Bed," PhD Dissertation, University of Southern California, Los Angeles, CA, USA, 2011.

[11] K.J. Bathe, and E.L. Wilson, Numerical Methods in Finite Element Analysis, 2nd Ed., John Wiley and Sons, 1976.

[12] C.H. Ih, H.C. Briggs, S.J. Wang, "3D Dynamic Modeling and Simulation of a Precision Segmented Reflector Telescope", Proceedings of the 21st Annual Pittsburgh Conference, 1990.

[13] H. Ryaciotaki-Boussalis, H.C. Briggs, and C.H. Ih, "Dynamic Performance Modeling and Stability Analysis of a Segmented Reflector Telescope," Proceedings of the 1991 Automatic Control Conference, pp. 1705-1706, 1991.

[14] A.C. Carrier, "Modeling and Shape control of a Segmented-Mirror Telescope," Ph.D. dissertation, Dept. Aeronautics and Astronautics, Stanford Univ., Stanford, CA, 1990.

[15] R.D. Cook, Concepts and Applications in Finite Element Analysis, 2nd Ed., John Wiley and Sons, 1981.

[16] R. Bishop, and D.C. Johnson, The Mechanics of Vibration, Cambridge University Press, 1981.